Chemical Papers
https://doi.org/10.1007/s11696-021-01707-7

ORIGINAL PAPER

Discovery of pyrazole derivatives as potent inhibitor of NF-κB for possible benefit in abdominal aortic aneurysms

Yun Guo[1] · Dongming Bao[1] · Chaogang Zhang[1]

Received: 17 December 2020 / Accepted: 18 May 2021

Abstract
Numerous 3-(4-substitutedyphenyl)-5-methyl-1-phenyl-1*H*-pyrazole-4-carboxylate derivatives have been synthesized using $H_2SO_4.SiO_2$ as a catalyst. These derivatives were subsequently screened for NF-κB transcription inhibitory activity in RAW264.7 cells, where they showed mild to significant inhibition. Among the tested derivatives, Compound 4e was identified as a most potent NF-κB transcription inhibitor. The effect of compound 4e was further studied in abdominal aortic aneurysm (AAA) animal model in BALB/c mice. The AAA was induced in mice by sub-cuteneous administration of Angiotensin-II (Ang-II). Results suggest that compound 4e significantly inhibited inflammation and oxidative stress in AAA mice as compared to disease control. It also inhibits NF-κB and COX-2 in AAA mice as shown by western blot analysis. Collectively, it was concluded that, compound 4e might acts as protective agent against AAA.

Keywords Pyrazole · One-pot synthesis · Silica · NF-κb · COX-2

Introduction:

Abdominal aortic aneurysm (AAA) is a life threatening dwindling illness which often leads to death of the patient if not treated well in time. The exact diagnosis of AAA is quite cumbersome process due to its asymptomatic behaviour until the rupture of aorta occurs. The AAA can be characterised by the expansion of abdominal aortic diameter by 50% of the original (Keisler and Carter 2015). The recent epidemiological data suggests that men aged more than 65 year are more prone to this illness and approximately 80% of the mortality of this disease is due to rupture of aorta. The current therapeutic modality to treat AAA is entirely based on reconstructive surgery if the aortic diameter is over 5.5 cm (Aggarwal et al. 2011; Setacci et al. 2016). However, there is no medication for the patients with small AAA, as surgery is fruitful only in major AAA. Thus, is worthwhile to discover new agents for small AAA.

Various studies have confirmed the role of inflammation in the development and progression of AAA. It is temporally and spatially linked with disorder of the orderly lamellar arrangement of the aortic media. The human AAA tissue showed higher expression of inflammatory infiltrates in both the media and adventitia (Freestone et al. 1995; Shimizu et al. 2006). Nuclear factor (NF)-kappaB (NF-κB), a transcription factor responsible for controlling the action of various genes linked with inflammatory response in AAA (Saito et al. 2013). It is found aberrantly activated in many experimental studies of AAA to promote chronic inflammation of aortic walls, activation of MMPs (matrix metalloproteases) and degradation of extra cellular matrix (ECM) (Raffetto and Khalil 2008; Rabkin 2017).

Pyrazole, a privileged heterocyclic scaffold associated with numerous pharmacological activities ranging from anti-infective agents to treat lifestyle diseases, such as cardiovascular, diabetes (Faria et al. 2017). Various studies have shown strong anti-inflammatory activity of pyrazole by inhibiting COX-2 and NF-κB in micro to nano-molar range (Abdelgawad et al. 2017; Hassan et al. 2019),(Pippione et al. 2018; Masih et al. 2020b). The clinical significance of pyrazole against inflammation is understood by the fact that, some of the best anti-inflammatory agents are derived from pyrazole nucleus, such as, Celecoxib (Gong et al. 2012), Lonazolac (Raulf and König 1990) and Mepirizole (Boonyaratavej 1979; Tanaka et al. 1989). However, the synthesis of substituted pyrazole is quite tedious and difficult process due to involvement

✉ Yun Guo
17358507362m@sina.cn

[1] Department of Interventional, Qionglai Medical Center Hospital, Qionglai 611530, Sichuan, China

Published online: 30 May 2021

of multi-step reaction and associated purification, low yield and complex workup. In this regard, various scientist have developed facile synthesis of pyrazole to tackle above-mentioned drawback by one-pot multi-step reaction using numerous catalysts, such as, sodium ascorbate (Kiyani and Bamdad 2018), molecular iodine (Mahdavi et al. 2016), ionic liquid (Singh et al. 2013), nanoparticle (Ghorbani-Vaghei et al. 2017), graphene oxide-phosphoric acid (Zakeri et al. 2019). In a report by Jawale et al. they have synthesized some pyrazole derivatives using SSA as a catalyst in a facile and excellent yield (Jawale et al. 2011). Therefore, in the present study, we have employed same methodology for the synthesis of numerous pyrazoles using SSA as a catalyst for potential benefit in AAA.

Experimental

Chemistry

The chemicals used in the present study were obtained from Sigma-Aldrich (USA). ^{1}H NMR spectra were recorded in DMSO-*d6* on a Bruker Avance-400 NMR spectrometer with TMS as the internal reference. ^{13}C NMR spectra were recorded on a Bruker Avance-100 NMR spectrometer in DMSO-*d*6 on the same spectrometers with TMS as the internal reference. The multiplicity of a signal is indicated as: s – singlet, d – doublet, t – triplet, q – quartet, m – multiplet, br – broad, dd – doublet of doublets. Coupling constants (*J*) are quoted in Hz and reported to the nearest 0.1 Hz. Infrared spectra were recorded as a neat thin film on a Perkin-Elmer Spectrum One FT-IR spectrometer using Universal ATR sampling accessories. Melting points were obtained using MEL-TEMP (model 1001D). MS spectra were recorded on an Agilent 1100 LC/MS. Elemental analysis was performed with Vario elemental analyser and were in agreement with the proposed structures within ± 0.4% of the theoretical values.

Synthesis of H_2SO_4·SiO_2

The synthesis of sulfuric acid adsorbed on silica gel was performed with the earlier reported procedure, where silica gel (29.5 g, 230–400 mesh size) was suspended in ethyl acetate (60 mL) and then H_2SO_4 (1.5 g, 15.5 mmol, 0.8 mL of a 98% aq. solution of H_2SO_4) was added to the above mixture. The whole mixture was stirred magnetically for 30 min at rt and after stirring the ethyl acetate was removed under reduced pressure. The resulting mass was heated under vacuum for 72 h at 100–120 °C under vacuum to afford H_2SO_4–SiO_2 as a free flowing powder.

General procedure for the synthesis of substituted pyrazole 4 (a-g)

Aromatic aldehyde (**1**, 1 mmol), phenyl hydrazine (**2**, 1 mmol) and ethyl acetoacetate (**3**, 1 mmol) was mixed together. To this above mixture H_2SO_4–SiO_2 (15 mol%) was added at room temperature for the appropriate time as ascertained with the help of TLC. The reaction mixture after the completion of reaction was diluted with EtOAc (20 ml), filtered, water (30 ml) added, the solution extracted with EtOAc (3 × 15 ml), and the combined organic layers were dried over anhydrous Na_2SO_4 and concentrated. The residue was subjected to column chromatography to obtain the pure desired product.

Ethyl 3-(4-hydroxyphenyl)-5-methyl-1-phenyl-1H-pyrazole-4-carboxylate (4e)

Yield: 89%; M.p: 176–178 °C; MW: 322.36; R_f (Benzene and Ethyl acetate 1:1): 0.69; FTIR (ν_{max}; cm^{-1} KBr): 3242 (O–H stretching), 3047 (Aromatic C-H stretching), 2945 (CH_2 stretching), 2874 (CH_3 stretching), 1716 (C = O stretching), 1635 (C = C stretching), 1573 (N–N stretching), 1462 (CH_3 bending), 1405 (COO stretching), 1372 (CH_2 bending), 1286 (C–O stretching), 1218 (C–N stretching), 784; ^{1}H-NMR (400 MHz, DMSO-*d*^{6}, TMS) δ ppm: δ 1.23 (t, 3H, *J* = 7.1 Hz, CH_3), 2.58 (s, 3H, CH_3), 4.08 (q, 2H, *J* = 7.1 Hz, CH_2), 7.23 (d, 2H,, J = 1.3 Hz, Ar–H), 7.41 (t, 1H, *J* = 1.3 Hz, Ar–H), 7.58 (d, 2H, J = 1.56 Hz, Ar–H), 7.62 (d, 2H, *J* = 1.86 Hz, Ar–H), 7.83 (d, 2H, *J* = 1.3 Hz, Ar–H), 9.59 (s, 1H, Ar-OH); ^{13}C-NMR (100 MHz, DMSO-d^{6}, TMS) δ ppm: 162.5, 158.6, 153.7, 144.9, 133.8, 129.4, 128.7, 126.2, 125.7, 124.8, 116.3, 110.8, 60.9, 14.1, 11.6; Mass: 323.36 (M + H) + ; Elemental analysis for $C_{19}H_{18}N_2O_3$: Calculated: C, 70.79; H, 5.63; N, 8.69.Found: C, 70.76; H, 5.67; N, 8.73.

Pharmacological activity

NF-kB transcription inhibitory activity

The entire synthesized compound (at 10 μM) was tested for their effect on the relative NF-κB transcriptional activity in RAW264.7 cells using Dual-Luciferase Reporter Assay System (Promega) as per the instruction provided by manufacturer.

In vivo *biological activity*

Angiotensin II-induced AAA mice model and treatment

The Male BALB/C male mice (n = 18) after procuring from the central animal house were kept in controlled temperature and humidity with alternate light and dark cycles mice. They were fed with laboratory diet and water ad libitum. The

following groups of mice were created for assessment of the role of compound **4e**.

Group 1: Control: Normal saline solution (0.5 mL, i.p.) daily for 4 weeks ($n = 6$).

Group 2: Angiotensin II-treated, (1,000 ng/kg/min angiotensin II, s.c.) + saline daily for 4 weeks (i.p.)

Group 3: Compound **4e** (25 mg/kg) suspended in 0.5% CMC i.p. daily for 4 weeks.

The mice was euthanized by an excess of anesthetic (500 µl 3% pentobarbital sodium; Sigma-Aldrich).

Estimation of angiotensin II-induced AAA mice

The periadventitial tissue from the aortic wall was removed after fixing aorta 4% cold paraformaldehyde by using dissecting microscope. The aorta was macroscopically examined to record maximal external diameter of the suprarenal aorta using MultiGuage 3000 imaging processing software. The state of aortic aneurysm was achieved when the aortic outer diameter was found enlarged > 50%.

Measurement of inflammation

TNF-α, IL-1β and IL-6 serum levels were determined using the eBioscience mouse ELISA antibody set. Absorbance was determined at 450 nm wavelength using an ELISA reader (Spectramax Plus, Molecular Devices, LLC, Sunnyvale, CA, USA).

Western blot analysis of NF-κB and COX-2

The isolated protein from the whole aorta was probed to 10% SDS-PAGE for 50 min and transferred to PVDF membrane. The membrane was blocked with 5% defat milk in tris-buffered saline with 0.1% Tween 20 for 1 h at 4 °C and then incubated with rabbit anti-mouse NF-κB, COX-2 (1:1,000), and β-actin (1:2,000) primary antibodies at 4 °C for overnight. Afterwards, the membrane was incubated with anti-mouse IgG HRP-conjugated secondary antibodies (1:5000). Protein expression was detected with an enhanced chemiluminescence detection kit.

Docking

The 3D X-ray crystal structure of transcription factor NK-kappa B p50 homodimer bound to a palindromic kappa B site was used as a target protein model for this study (1nfk.pdb). All computational analyses were carried out using Discovery Studio 3.5.

Preparation of receptor The water was removed from the protein, and the bond orders were corrected. The hydrogen atoms were added, their positions optimized using the all-atom CHARMm (version c32b1) forcefield with Adopted Basis set Newton Raphson (ABNR) minimization algorithm until the root mean square (r.m.s) gradient for potential energy was less than 0.05 kcal/mol/Å. Using the 'Binding Site' tool panel available in DS 3.5, the minimized transcription factor NK-κB p50 homodimer bound to a palindromic κB site was defined as receptor, and the largest cavity was selected as a binding site for docking runs. The centre of the sphere was created around the identified binding site, and side chains of the residues in the binding site within the radius of the sphere were assumed to be flexible during refinement of post-docking poses.

Ligand setup Using the built-and-edit module of DS 3.5, the compound 4e was built, all-atoms CHARMm forcefield parameterization assigned and then minimized using the ABNR method. A conformational search of the ligand was carried out using a stimulated annealing molecular dynamics (MD) approach. The ligand was heated to a temperature of 700 K and then annealed to 200 K. Thirty such cycles were carried out. The transformation obtained at the end of each cycle was further subjected to local energy minimization, using the ABNR method. The 30 energy-minimized structures were then superimposed and the lowest energy conformation occurring in the major cluster was taken to be the most probable conformation.

Docking and scoring

CDOCKER protocol of DS 2.5 was used for the docking of compound 4e with transcription factor NK-κB p50 homodimer bound to a palindromic κB site. The receptor protein conformation was kept fixed during docking, and the docked poses were further minimized using all-atom CHARMm (version c32b1) forcefield and smart minimization method (steepest descent followed by conjugate gradient) until r.m.s gradient for potential energy was less than 0.05 kcal/mol/Å. The atoms of ligand and the side chains of the residues of the receptor within 5 Å from the centre of the binding site were kept flexible during minimization. Finally, the best docked pose of compound **4e** was analysed for it interaction with receptor protein using the Visualizer of the software.

Statistical analysis

Data are presented as means ± standard error Statistical analysis was performed using Student's t-test for paired or unpaired data, and data were assessed using Graphpad Prism (version 5). $P < 0.05$ was considered to indicate a statistically significant difference.

Scheme 1 Synthesis of pyrazole derivatives **4 (a-g)**

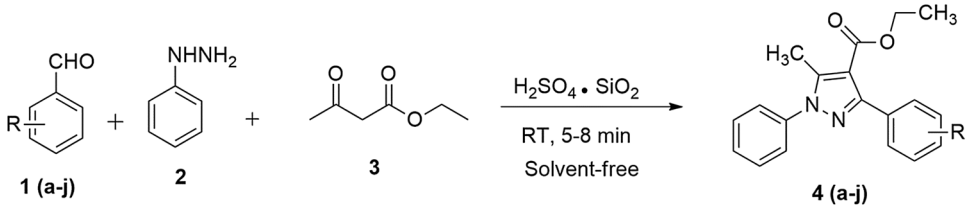

Table 1 Effect of catalyst loading on the reaction

Entry	H_2SO_4·SiO_2 (in mol %)	Time (in min)	Yield (in %)[b]
1	5	650	30
2	10	265	47
3	15	31	92
4	20	19	60

[a]Reaction conditions: Benzaldehyde (1 mmol), phenylhydrazine (1 mmol), and ethyl acetoacetate (1 mmol); catalyst, room temperature, solvent free

[b]Isolated and unoptimized yield

Table 2 Effect of Temperature on the reaction condition

Entry	Temperature (in C°)	Time (in min)	Yield (in %)[b]
1	10	1260	23
2	Room temperature	31	92
3	50	20	62
4	100	11	40
5	140	6	32

[a]Reaction conditions: Benzaldehyde (1 mmol), phenylhydrazine (1 mmol), and ethyl acetoacetate (1 mmol); $H2SO_4$·SiO_2 (15 mol %), solvent free

[b]Isolated and unoptimized yield

Results and discussion

Synthesis of Target molecules 4 (a-j)

The synthesis of pyrazole derivatives has been achieved using catalyst (H_2SO_4.SiO_2, silica-supported sulfuric acid), Scheme 1. Initially, the optimal catalyst loading of silica-supported sulfuric acid catalyst for the reaction was identified using benzaldehyde, phenylhydrazine and ethylacetoacetate in equi-molar quantity as a model reaction. As shown in Table 1, at the initial catalytic load of 5 mol %, the product yield was found lowest, the product conversion being only 30% in approximately 11 h, the longest reaction time (Table 1, entry 1). The twofold increment of the catalytic load to 10% (Table 1, entry 2) showed marked improvement in the reaction time with marginal increment in the product yield. The highest conversion of the product was observed at 15 mol % catalyst loading with subsequent reduction in the reaction time (Table 1, entry 3). A further increase in catalyst load (20 mol %) seems to hamper the reaction as suggested by significant reduction in the product yield, albeit it improves the reaction time (Table 4). Thus, based on the above observation, 15 mol % is identified as an optimal catalyst load for the efficient synthesis of pyrazole. The reaction conditions were further optimized studying the effect of the temperature on the catalytic efficiency and product yield using the same model reaction template. As shown in Table 2, at 10 °C, the reaction took maximum time to complete with the least product yield. However, the maximum product yield was obtained at the reaction conducted at the room temperature which took nearly 30 min to complete. In the next runs (Table 2, entry 3, 4 and 5), it was marked to note that reaction took shorter time to afford the product upon increasing the temperature, however, it does not found favourable to the product yield, which found significantly reduced as the temperatures rises. Thus, reaction conducted at room temperature seems favourable as compared to the other temperature conditions. Recyclability/reusability of catalyst is a vital point which needs to be considered for the applicability of the catalyst for any reaction. The reusability of a catalyst has a significant impact in terms, limiting waste generation, economically viable, and environment friendly. Thus, in the next instance, the recyclability of the catalyst was then evaluated. The catalyst was recovered by filtration, washed with ethyl acetate (10 mL), dried and reused for a further catalyzing the reaction. As shown in Table 3, the catalyst can be used for six-consecutive runs without much loss of ability. However, the significant reduction in product yield was obtained in seventh-run of catalyst reusability. Thus, it could be suggested that catalyst can be recovered and reused for 6 cycles at least, fully preserving its activity and selectivity. On the basis of the above observation, it could be suggested that, 15 mol % loading of the catalyst at a room temperature was efficient to catalyze the reaction with maximum yield.

Finally, with optimized conditions in our hands, we checked the scope of this catalytic methodology for the synthesis of substituted pyrazole using numerous electron-donating and withdrawing substituents as a starting material. As shown in Table 4, the compounds containing electron-withdrawing group were obtained in excellent yield as

Table 3 Recyclability of catalyst for reaction

Entry	Yield (in %)[b]	Run
1	92	1
2	92	2
3	92	3
4	91	4
5	90	5
6	89	6
	68	7

[a]Reaction conditions: Benzaldehyde (1 mmol), phenylhydrazine (1 mmol), and ethyl acetoacetate (1 mmol); $H_2SO_4{\cdot}SiO_2$ (15 mol %), room temperature, solvent free

[b]Isolated and unoptimized yield

compared to their electron donating counterparts. Moreover, compound with no-substitution showed highest yield among the synthesized derivatives. The formation of pyrazoles was established on the basis of a melting point which was found in the agreement with earlier reported literature (Meng et al. 2016).

NF-κB Transcriptional inhibition activity

The synthesized pyrazole derivative **4** (**a-g**) were evaluated for relative NF-κB transcriptional activity in LPS stimulated RAW264.7 cells. As shown in Table 5, entire set of compounds displayed significant to moderate NF-κB transcriptional inhibitory activity. The compound **4a** showed least NF-κB transcriptional inhibitory activity. The inhibitory activity was considerably improved on the introduction *chloro* group (**4b**). The replacement of *chloro* with the *fluoro* (**4c**) showed reduced activity. However, no significant change in activity was reported by the introduction of bromo (**4d**) in place of fluoro. The activity was significantly increased upon the insertion of hydroxy (**4e**) which render compound highly potent among the tested derivatives. The inhibitory activity was further found reduced upon introduction of methoxy (**4f**) and methyl (**4g**). On close inspection of comparative inhibitory activity of tested derivatives, compound **4e** found highly active among the tested derivatives showing approximately similar inhibitory activity to Celecoxib as a standard.

Table 5 Effect of compound **4 (a-g)** on NF-κB transcriptional activity in LPS-stimulated RAW264.7 cells

Compound	Substituent	Relative NF-κB transcriptional activity (NF-κB/TK, fold)[a]
4a	H	$5.03 \pm 1.05^{\#}$
4b	4-Cl	$3.76 \pm 1.32^{\#}$
4c	4-F	$4.87 \pm 0.97^{\#}$
4d	4-Br	$4.80 \pm 0.69^{\#}$
4e	4-OH	$1.34 \pm 0.47^{\#}$
4f	4-OCH_3	$2.45 \pm 0.36^{\#}$
4 g	4-CH_3	$3.02 \pm 1.02^{\#}$
Celecoxib		1.82 ± 0.21
Control		0.39 ± 0.07
LPS		$5.67 \pm 0.95^{**}$

LPS, lipopolysaccharide; *NF-κB*, nuclear factor kappa B

N = 3

[a]At 10 μM

$^{\#}P < .01$ versus LPS

$^{**}P < .01$ versus control

Pharmacological activity of Compound 4e against abdominal aortic aneurysm (AAA) in mice

Impressed by the potent NF- κB transcriptional effect of compound **4e**, in the next part, we aimed to investigate whether compound **4e** has any effect on abdominal aortic aneurysm in the rats. The AAA in mice was induced by administration of angiotensin II (Ang-II). Various studies have shown a clear link between Ang-II and AAA, where

Table 4 Synthesis of pyrazole derivatives **4** (**a-j**)

Entry	Substituent	Yield (in %)	M.P. (in °C, found)	M.P. (in °C, reported) (Meng et al. 2016)
4a	H	92	142–144	143–144
4b	4-Cl	90	175–178	176–177
4c	4-F	90	109–112	110–111
4d	4-Br	91	175–178	178–179
4e	4-OH	86	176–178	178–179
4f	4-OCH_3	85	124–128	124–125
4 g	4-CH_3	87	172–175	175–176

[a]Reaction conditions: Substituted Benzaldehyde (1 mmol), phenylhydrazine (1 mmol), and ethyl acetoacetate (1 mmol); $H_2SO_4{\cdot}SiO_2$ (15 mol%), room temperature, solvent free

it causes induction VCAM-1 expression by activating NF-κB–dependent gene expression. In addition, Ang-II stimulates production of reactive oxygen species (ROS) by inducing a vascular NADH oxidase (Daugherty et al. 2000; Golledge et al. 2006; Weintraub 2009; Cao et al. 2010). As shown in Fig. 1, the mice treated with Ang-II showed higher incidence of AAA in mice together with high mortality and max aortic aneurysm as compared to control. However, upon administration of compound **4e** (25 mg/kg) showed significant reduction in these indices as compared with Ang-II model group. The effect of compound **4e** was then investigated on the level of various pro-inflammatory cytokines (TNF-α, IL-1β and IL-6) in AAA mice. As shown in Fig. 2, the level of these cytokines was found elevated in AAA-model group as compared to control, whereas, their level were found significantly reduced in compound **4e** treated mice. Oxidative stress is the characteristic hallmark of AAA (McCormick et al. 2007; Kuivaniemi et al. 2015). Thus, the effect of compound **4e** was investigated on the level of various biomarkers of oxidative stress in AAA mice, such as MDA, SOD and GSH. It has been found that compound **4e** causes significant reduction in MDA content and increases SOD and GSH activity (Fig. 3). Various studies showed excellent correlation between the higher expressions NF-κB and COX-2 and incidence of AAA (Guo et al. 2006). Thus, the effect of compound **4e** was further investigated on the expression of NF-κB and COX-2 using western blot analysis. As shown in Fig. 4, compound **4e** significantly reduces the expression of both NF-κB and COX-2 in AAA rats.

Molecular docking analysis of compound 4e with NF-κB

Now days, molecular docking has attracted wide attention from scientists across the globe working on drug discovery. It is a powerful tool that can able to predict the 3D-alignment of ligand into the active site of receptor of interest which allows us to illustrate the action of small molecules into the binding site of aimed proteins as well

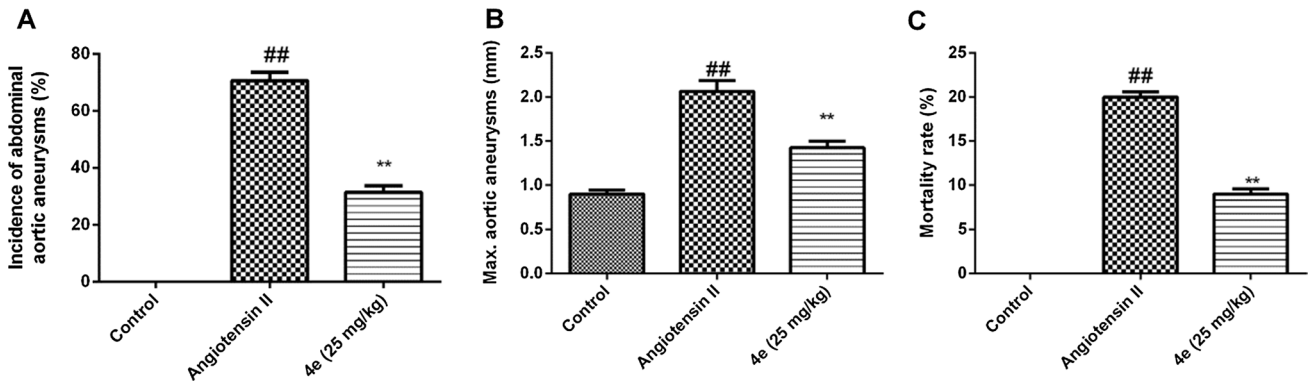

Fig. 1 Effect of compound **4e** (25 mg/kg) on the indices of abdominal aortic aneurysms in rats induced by Angiotension-II. **a** incidence of abdominal aortic aneurysms, **b** max. aortic aneurysms, and **c** mortality rate. $^{\#\#}P < 0.01$ *vs.* the control group and $^{**}P < 0.01$ *vs.* the angiotensin II group. Data are presented as means ± SEM

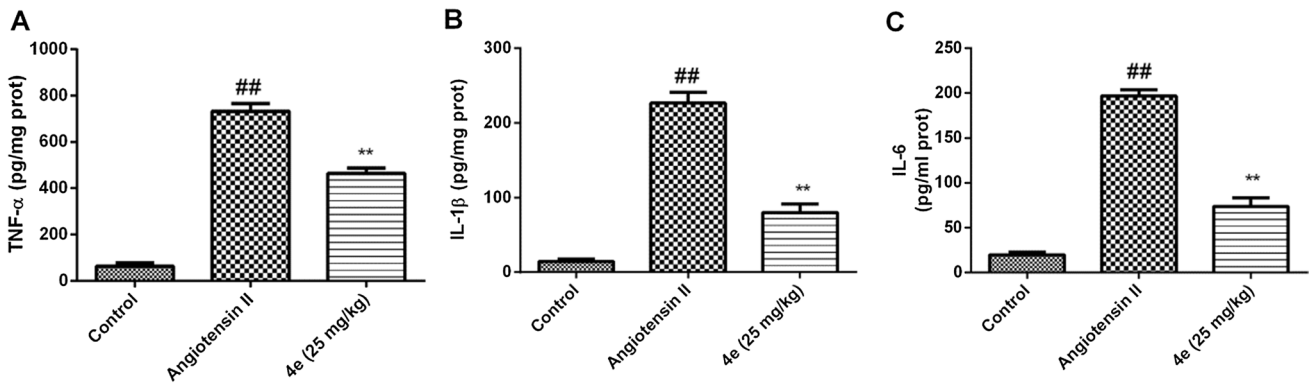

Fig. 2 Effect of compound **4e** (25 mg/kg) on various pro-inflammatory cytokines in abdominal aortic aneurysms in rats induced by Angiotension-II. **a** TNF-α, **b** IL-1β, and **c** IL-6. $^{\#\#}P < 0.01$ *vs.* the control group and $^{**}P < 0.01$ versus the angiotensin II group. Data are presented as means ± SEM

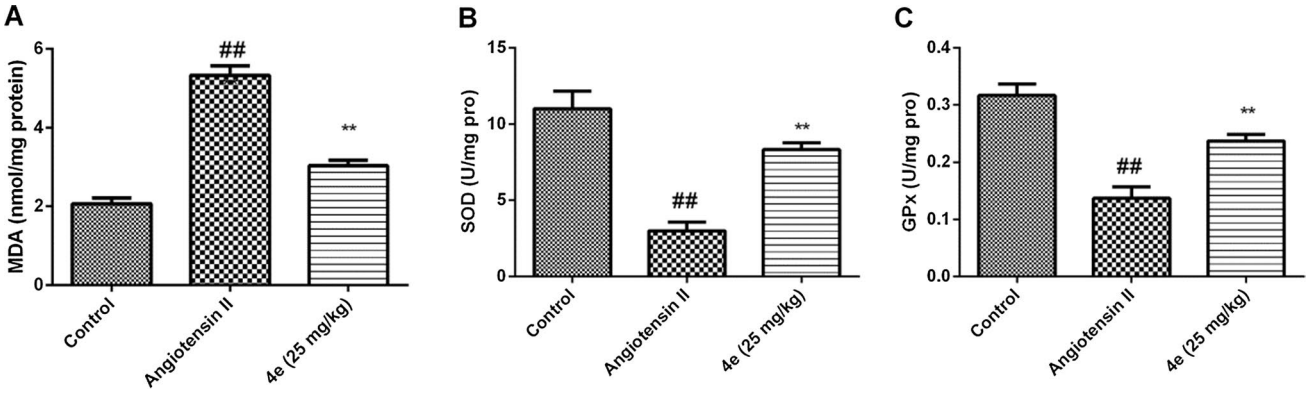

Fig. 3 Effect of compound **4e** (25 mg/kg) on various indices of oxidative stress in abdominal aortic aneurysms in rats induced by Angiotension-II. **a** MDA, **b** SOD, and **c** GPx. $^{\#\#}P<0.01$ *vs.* the control group and $^{**}P<0.01$ versus the angiotensin II group. Data are presented as means ± SEM

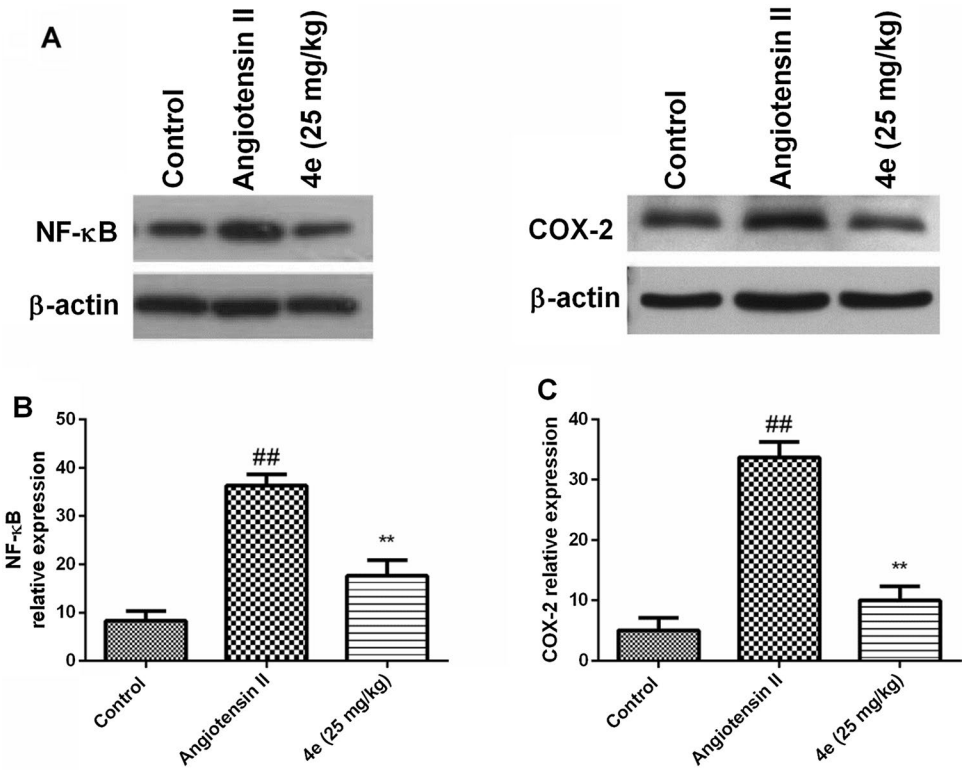

Fig. 4 Effect of compound **4e** (25 mg/kg) on various pro-inflammatory cytokines in abdominal aortic aneurysms in rats induced by Angiotension-II. **a** TNF-α, **b** IL-1β, and **c** IL-6. $^{\#\#}P<0.01$ *vs.* the control group and $^{**}P<0.01$ versus the angiotensin II group. Data are presented as means ± SEM

as to explicate elementary biochemical processes (Meng et al. 2012; Sliwoski et al. 2014). Therefore, encouraged by the excellent inhibitory activity of compound **4e** in the both *in-vitro* and *in-vivo* experiments, we envisage to perform molecular docking experiment of **4e** with 3D-crystal structure of NF-κB. Results of the docking study presented in Figs. 5 and 6. It has been found that compound **4e** created numerous interactions into the active site of NF-κB by creating inter-atomic contacts with neighbouring amino acid residues (shown in color coded form in Fig. 6). The oxygen atom of ketone and hydroxy group and pyrazole Nitrogen atom of compound **4e** showed formation of van der Waals and Hydrogen bond with Lys145 of Chain A and B and Thr143 of Chain B. Moreover, the methyl of compound **4e** interacted with Cys59 of Chain A of receptor via alkyl bond. Two pi-alkyl interactions was reported by phenyl linked to Nitrogen atom of pyrazole with Lys146 and Val58 of Chain B of the NF-κB. The interaction shown by compound **4e** found similar with earlier reported results

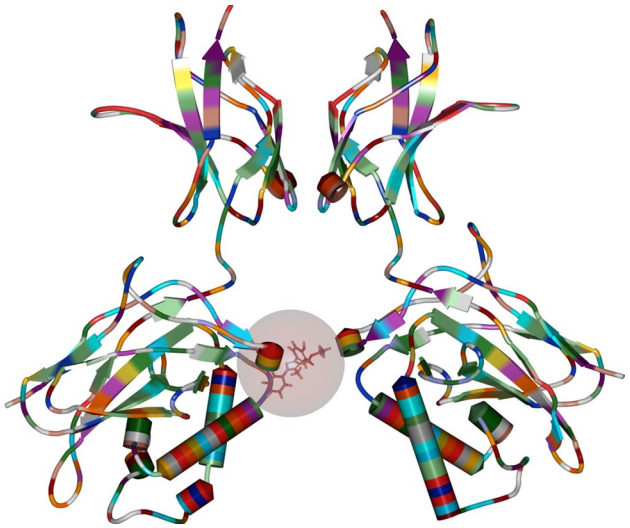

Fig. 5 Docked orientation of compound **4e** into the active site of NF-κB 3D-crystal structure identified by molecular docking analysis

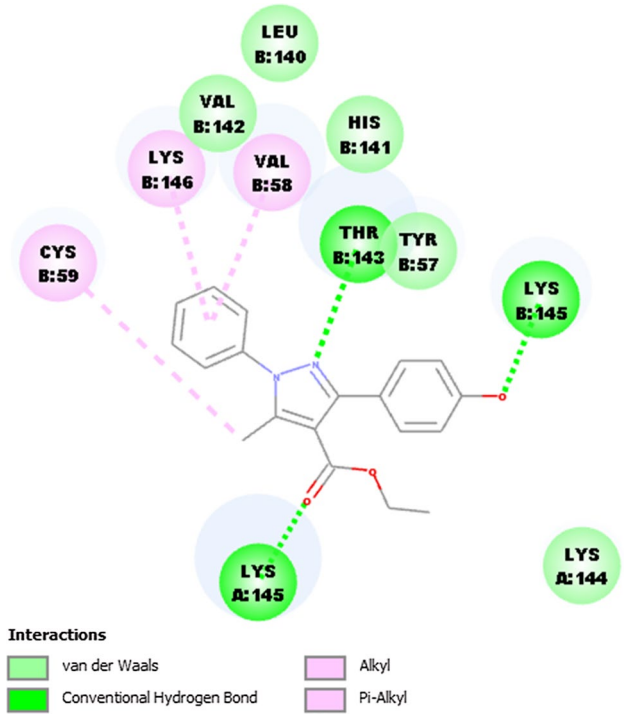

Fig. 6 2D interaction of docked pose of compound **4e** into the active site of NF-κB showing neighbouring interacting residues

(Srivastava et al. 2015; Masih et al. 2020a). Thus, it could be suggested that compound **4e** might exert potent inhibitor of NF-κB transcription activity due to strong interaction with catalytic residues of NF-κB protein.

Conclusion

Our study demonstrated the usefulness of synthesized pyrazole. The compounds found excellent inhibitor of NF-κB and showed protective effect against aortic aneurysms via inhibition of oxidative stress and inflammation. However, much studies are need on these derivative make them viable lead for clinical use.

Declarations

Conflict of interest The authors declare that they have no conflict of interest.

References

Abdelgawad MA, Bakr RB, Omar HA (2017) Design, synthesis and biological evaluation of some novel benzothiazole/benzoxazole and/or benzimidazole derivatives incorporating a pyrazole scaffold as antiproliferative agents. Bioorg Chem 74:82–90. https://doi.org/10.1016/j.bioorg.2017.07.007

Aggarwal S, Qamar A, Sharma V, Sharma A (2011) Abdominal aortic aneurysm: A comprehensive review. Exp Clin Cardiol 16:11–15

Boonyaratavej N (1979) Clinical evaluation of mepirizole. J Med Assoc Thail 62:682–685

Cao RY, St Amand T, Ford MD et al (2010) The murine angiotensin II-induced abdominal aortic aneurysm model: Rupture risk and inflammatory progression patterns. Front Pharmacol. https://doi.org/10.3389/fphar.2010.00009

Daugherty A, Manning MW, Cassis LA (2000) Angiotensin II promotes atherosclerotic lesions and aneurysms in apolipoprotein E-deficient mice. J Clin Invest 105:1605–1612. https://doi.org/10.1172/JCI7818

Faria JV, Vegi PF, Miguita AGC et al (2017) Recently reported biological activities of pyrazole compounds. Bioorganic Med Chem 25:5891–5903

Freestone T, Turner RJ, Coady A et al (1995) Inflammation and matrix metalloproteinases in the enlarging abdominal aortic aneurysm. Arterioscler Thromb Vasc Biol 15:1145–1151. https://doi.org/10.1161/01.ATV.15.8.1145

Ghorbani-Vaghei R, Mahmoodi J, Shahriari A, Maghbooli Y (2017) Synthesis of pyrano[2,3-c]pyrazole derivatives using Fe3O4@SiO2@piperidinium benzene-1,3-disulfonate (Fe3O4@SiO2 nanoparticle-supported IL) as a novel, green and heterogeneous catalyst. Appl Organomet Chem. https://doi.org/10.1002/aoc.3816

Golledge J, Muller J, Daugherty A, Norman P (2006) Abdominal aortic aneurysm: Pathogenesis and implications for management. Arterioscler Thromb Vasc Biol 26:2605–2613

Gong L, Thorn CF, Bertagnolli MM et al (2012) Celecoxib pathways: pharmacokinetics and pharmacodynamics. Pharm Genomics 22:310–318

Guo DC, Papke CL, He R, Milewicz DM (2006) Pathogenesis of thoracic and abdominal aortic aneurysms. Ann N Y Acad Sci 1085:339–352

Hassan GS, Abdel Rahman DE, Abdelmajeed EA et al (2019) New pyrazole derivatives: Synthesis, anti-inflammatory activity,

cycloxygenase inhibition assay and evaluation of mPGES. Eur J Med Chem 171:332–342. https://doi.org/10.1016/j.ejmech.2019.03.052

Jawale DV, Pratap UR, Mali JR, Mane RA (2011) Silica chloride catalyzed one-pot synthesis of fully substituted pyrazoles. Chin Chem Lett 22:1187–1190. https://doi.org/10.1016/j.cclet.2011.05.016

Keisler B, Carter C (2015) Abdominal aortic aneurysm. Am Fam Phys 91:538–543

Kiyani H, Bamdad M (2018) Sodium ascorbate as an expedient catalyst for green synthesis of polysubstituted 5-aminopyrazole-4-carbonitriles and 6-amino-1,4-dihydropyrano[2,3-c]pyrazole-5-carbonitriles. Res Chem Intermed 44:2761–2778. https://doi.org/10.1007/s11164-018-3260-0

Kuivaniemi H, Ryer EJ, Elmore JR, Tromp G (2015) Understanding the pathogenesis of abdominal aortic aneurysms. Expert Rev Cardiovasc Ther 13:975–987

Mahdavi M, Khoshbakht M, Saeedi M et al (2016) Iodine-Mediated Synthesis of Novel Pyrazole Derivatives. Synth 48:541–546. https://doi.org/10.1055/s-0035-1560553

Masih A, Agnihotri AK, Srivastava JK et al (2020a) Discovery of novel pyrazole derivatives as a potent anti-inflammatory agent in RAW264.7 cells via inhibition of NF-κB for possible benefit against SARS-CoV-2. J Biochem Mol Toxicol. https://doi.org/10.1002/jbt.22656

Masih A, Agnihotri AK, Srivastava JK, et al (2020b) Discovery of novel pyrazole derivatives as a potent anti-inflammatory agent in RAW264.7 cells via inhibition of NF-κB for possible benefit against SARS-CoV-2. J Biochem Mol Toxicol 35: e22656.

McCormick ML, Gavrila D, Weintraub NL (2007) Role of oxidative stress in the pathogenesis of abdominal aortic aneurysms. Arterioscler Thromb Vasc Biol 27:461–469

Meng X-Y, Zhang H-X, Mezei M, Cui M (2012) Molecular Docking: a powerful approach for structure-based drug discovery. Curr Comput Aided-Drug Des 7:146–157. https://doi.org/10.2174/157340911795677602

Meng FJ, Sun T, Dong WZ et al (2016) Discovery of novel pyrazole derivatives as potent neuraminidase inhibitors against influenza H1N1 virus. Arch Pharm (weinheim) 349:168–174. https://doi.org/10.1002/ardp.201500342

Pippione AC, Sainas S, Federico A et al (2018) N -Acetyl-3-aminopyrazoles block the non-canonical NF-kB cascade by selectively inhibiting NIK. Medchemcomm 9:963–968. https://doi.org/10.1039/c8md00068a

Rabkin SW (2017) The role matrix metalloproteinases in the production of aortic aneurysm. Prog Mol Biol Transl Sci 147:239–265

Raffetto JD, Khalil RA (2008) Matrix metalloproteinases and their inhibitors in vascular remodeling and vascular disease. Biochem Pharmacol 75:346–359. https://doi.org/10.1016/j.bcp.2007.07.004

Raulf M, König W (1990) Effects of the nonsteroidal anti-inflammatory compounds Lonazolac Ca, indomethacin and NDGA on inflammatory mediator generation and release from various cells. Immunopharmacol 19:103–111. https://doi.org/10.1016/0162-3109(90)90045-G

Saito T, Hasegawa Y, Ishigaki Y et al (2013) Importance of endothelial NF-κB signalling in vascular remodelling and aortic aneurysm formation. Cardiovasc Res 97:106–114. https://doi.org/10.1093/cvr/cvs298

Setacci F, Galzerano G, De DG et al (2016) Abdominal aortic aneurysm. J Cardiovasc Surg (torino) 57:72–85

Shimizu K, Mitchell RN, Libby P (2006) Inflammation and cellular immune responses in abdominal aortic aneurysms. Arterioscler Thromb Vasc Biol 26:987–994

Singh J, Srivastava M, Rai P, Singh J (2013) An environmentally friendlier approach—ionic liquid catalysed, water promoted and grinding induced synthesis of highly functionalised pyrazole derivatives. RSC Adv 3:16994–16998. https://doi.org/10.1039/c3ra42493f

Sliwoski G, Kothiwale S, Meiler J, Lowe EW (2014) Computational methods in drug discovery. Pharmacol Rev 66:334–395

Srivastava JK, Awatade NT, Bhat HR et al (2015) Pharmacological evaluation of hybrid thiazolidin-4-one-1,3,5-triazines for NF-κB, biofilm and CFTR activity. RSC Adv 5:88710–88718. https://doi.org/10.1039/c5ra09250g

Tanaka H, Nakagawa M, Takeuchi K, Okabe S (1989) Effects of mepirizole and basic antiinflammatory drugs on HCl-ethanolinduced gastric lesions in rats. Dig Dis Sci 34:238–245. https://doi.org/10.1007/BF01536058

Weintraub NL (2009) Understanding abdominal aortic aneurysm. N Engl J Med 361:1114–1116. https://doi.org/10.1056/nejmcibr0905244

Zakeri M, Abouzari-lotf E, Miyake M et al (2019) Phosphoric acid functionalized graphene oxide: a highly dispersible carbon-based nanocatalyst for the green synthesis of bio-active pyrazoles. Arab J Chem 12:188–197. https://doi.org/10.1016/j.arabjc.2017.11.006